Revue Phys. Appl. 23 (1988) 1361-1368

AOÛT **1988**, PAGE 1361

Classification Physics Abstracts 62.20 - 61.70

# Plastic deformation down to 4.2 K of CoO single crystals and T.E.M. observation of dislocations

A. Dominguez-Rodriguez, J. Castaing (\*), H. Koisumi (1), and T. Suzuki (1)

Departamento de Optica e Instituto Ciencias Materiales Sevilla (C.S.I.C.) Facultad de Fisica, Apartado 1065, 41080 Sevilla, Spain

(1) Institute of Industrial Science, University of Tokyo, Roppongi, Minato-Ku, Tokyo 106, Japan

(Reçu le 24 septembre 1987, révisé le 18 mars 1988, accepté le 3 mai 1988)

Résumé. — On a déformé plastiquement CoO à 4,2 K par compression de monocristaux le long de (100). L'influence des conditions thermodynamiques de préparation des échantillons a été montrée. La structure des dislocations observée en microscopie électronique en transmission (TEM) n'est pas directement reliée à celle existant pendant la déformation à très basse température.

Abstract. — Plastic deformation of CoO has been performed at 4.2 K by compression of single crystals along (100). The influence of thermodynamic conditions of specimen preparation has been shown. The dislocation structure observed by transmission electron microscopy (TEM) is not directly related to the one existing during deformation at very low temperature.

### 1. Introduction.

Rocksalt structure single crystals show extensive plasticity down to low temperatures. Alkali halides have been deformed without failure at temperatures as low as 1.5 K [1]. Refractory oxides such as MgO, NiO, CoO displayed plasticity at 77 K [2], which corresponds to 0.025  $T_{\rm M}$ , 0.034  $T_{\rm M}$  0.037  $T_{\rm M}$  respectively  $(T_{\rm M} = \text{ melting temperature})$ . Recently MgO containing impurities was deformed down to 4.2 K  $(0.0014 T_{\rm M}) [1, 3].$ 

In this study, we have investigated the plasticity of cobalt oxide between 4.2 K and 300 K.

In previous works, CoO single crystals were found unusually strong [4] due to Co<sub>3</sub>O<sub>4</sub> precipitates [5]; these precipitates appeared in spite of the specimen air-quench, designed to avoid precipitation. We have performed new experiments on CoO after heat treatments designed for precipitate-free single crystals; specimens were deformed down to liquid helium temperature (4.2 K). Thin foils were then cut

### 2. Experimental techniques.

deformation mechanisms.

2.1 SPECIMEN PREPARATION. — Single crystals have been prepared in an arc image furnace from high purity powder. They were identical to those used in [4] and [5]. Specimens were cut as parallelopipeds  $(2.5 \times 2.5 \times 6 \text{ mm}^3)$  with  $\{100\}$  faces and compressed along their longest dimension. A few specimens were annealed at 1000 °C during one week, at a partial pressure of oxygen of  $10^{-7}$  atm. This ensures thermodynamic equilibrium during annealing. The specimens were furnace cooled at 20 K/mn. They entered the Co<sub>3</sub>O<sub>4</sub> phase field at about 550 °C, at least 300 °C lower than for annealing in air [4]. Optical and TEM observations did not reveal any Co<sub>3</sub>O<sub>4</sub> precipitates, contrary to the case of air-quenched crystals [5]. At 550 °C, point defect diffusivity is slow enough to prevent the formation of precipitates, which could be responsible for the strengthening of CoO single crystals.

to examine the dislocation structure in the transmission electron microscope (T.E.M.) and relate it to

<sup>(\*)</sup> Permanent address: Laboratoire Physique des Matériaux, CNRS Bellevue, 92195 Meudon Cedex, France.

REVUE DE PHYSIQUE APPLIQUÉE. — T. 23, N° 8, AOÛT 1988

2.2 MECHANICAL TESTING. — Tests were performed on as-grown as well as annealed specimens. They were made in compression at a constant strain rate of  $10^{-4}$  s<sup>-1</sup>. The flow stress was determined at several temperatures between 4.2 K and 300 K using an experimental set-up described in [6]. After yielding, the cross-head was stopped and stress relaxation was observed. The specimen was then cooled down, and deformation was resumed. Apparent activation volumes  $v^*$  were estimated from stress relaxations using the usual method for activation analysis [7].

2.3 Transmission **ELECTRON** MICROSCOPY. -TEM foils were cut parallel to {110} planes. The foils were mechanically polished with diamond paste  $(4 \mu m)$  from 250  $\mu m$  down to about 100  $\mu m$ . At this stage, a dimple was machined, using diamond paste  $(4 \mu m)$ , to reduce the central part of the specimen to 30-40 µm thickness. Ion thinning, with a cold stage, was used to bring the foil to electron transparency. A carbon coating was deposited to avoid electrical charge accumulation during TEM observations; specimens were placed in a liquid nitrogen cold stage. Since deformations were performed at 4.2 K, the use of cold stages intended to prevent any evolution of the microstructure under the beams, although the specimens had been brought to room temperature after the mechanical test. The Philips microscope was operated at 120 kV.

### 3. Results.

3.1 PLASTIC YIELDING. — The critical resolved shear stress  $\tau_{\rm c}$  has been determined for the {110} slip plane. Its dependence with temperature is shown in figure 1 for CoO submitted to various thermodynamic treatments. The hardest crystals correspond to specimens annealed in air at 1 200 °C and deformed by Castaing *et al.* [4]. The softest crystals were obtained after annealing at low  $pO_2$  (see Sect. 2.1), the as-grown ones being intermediate in strength (Fig. 1).

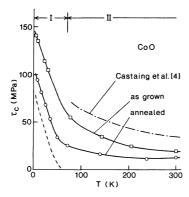


Fig. 1. — Critical resolved shear stress  $\tau_{\rm c}$  versus temperature T for CoO crystals having different thermodynamic treatments.

The temperature dependence of  $\tau_{\rm c}$  can be divided in two regions. In region I ( $T < 70~{\rm K}$ ),  $\tau_{\rm c}$  shows a variation with T much more rapid than in region II. The  $\tau_{\rm c}-T$  curves are roughly parallel in region I for the two kinds of crystals; the difference is about 40 MPa. Above 200 K,  $\tau_{\rm c}$  is almost independent of temperature (Fig. 1) as previously noted [4, 5].

The apparent activation volumes  $v^*$  are plotted in figure 2 for various temperatures. In region I,  $v^*$  is of the order of  $10 b^3$  and does not depend on the heat treatment of the crystals. Conversely, in region II, there is a marked dependence of  $v^*$  with heat treatments (Fig. 2). These results indicate that there is a major change in the mechanism controlling deformation from region I to II.

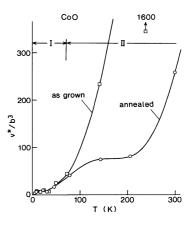
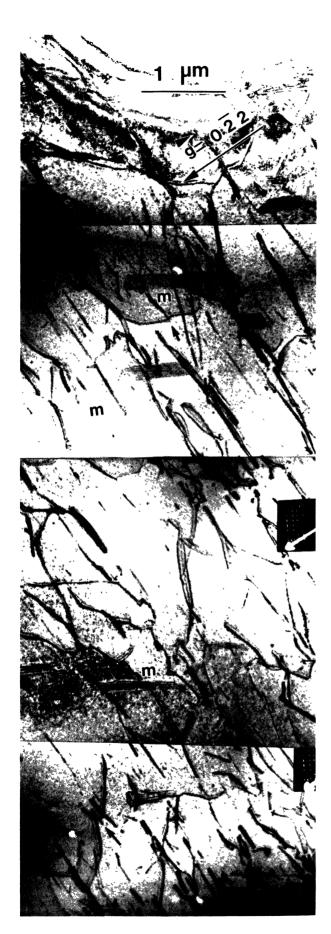


Fig. 2. — Apparent activation volume  $v^*$  in CoO determined by stress relaxation tests. b = 0.3 nm.

3.2 DISLOCATION MICROSTRUCTURE. — Foils were cut from a specimen shortened by 1% at 4.2 K. They were parallel to two orthogonal  $\{011\}$  and  $\{0\overline{1}1\}$  planes. For one orientation of cut, the foils contained dislocation dipoles, at an angle to the foil plane, which exhibited residual contrast. In the other orientation, extensive arrays of dislocations were observed (Fig. 3). At the T.E.M. scale, only one slip plane was activated. Since the observation was made at 77 K, magnetic domain walls can be seen (Fig. 3). They display similar contrast to those observed in NiO [8, 9].

An estimate of the dislocation density has been made, it is of the order of  $4 \times 10^8 \, \text{cm}^{-2}$ .

The Burgers vector was determined by usual  ${\bf g} \cdot {\bf b}$  analysis; there was no contrast for  ${\bf g}=311$  and 200, which is compatible with  ${\bf b}=\frac{1}{2}$   $\langle 0\overline{1}1 \rangle$ . In figure 3,  ${\bf b}$  is parallel to  ${\bf g}$ , it is easy to note that most dislocations have a strong edge character. They are arranged in dipoles and multipoles (Figs. 3, 4 and 5). These features are very similar to those observed in NaCl type crystals after deformation at moderate temperatures (0.2-0.4  $T_{\rm M}$ ) [2]. In some places, one



can observe configurations which could correspond to the mechanism of formation of dipoles by jog dragging (Fig. 3) or by collision of expanding loops (Fig. 5). An evaluation of dipole separation has been made by direct measurement on the micrographs. The most common value is 20 nm, average of values between 10 nm and 30 nm (Fig. 4).

#### 4. Discussion.

4.1 PLASTIC FLOW. — The plastic flow to CoO single crystals occurs by glide in the  $\{0\overline{1}1\}$   $\langle 011 \rangle$  system. The stress shows two remarkable features that we now discuss (i) strength which depends on the heat treatment (ii) strong thermal activation with two regions (Fig. 1).

Three kinds of specimens have been studied. They are characterized by various amont of  $\text{Co}_3\text{O}_4$  precipitates. As-grown crystals display large irregular precipitates [5] with an intermediate strength (Fig. 1). In order to control the thermodynamic parameters, crystals were annealed in air at  $1\,200\,^{\circ}\text{C}$ ; they contained a regular array of  $\text{Co}_3\text{O}_4$  precipitates [5]; they were very strong as long as tests were performed in the range of stability of  $\text{Co}_3\text{O}_4$  [4]. However, this hardening cannot be explained on the basis of dislocation precipitate interactions; the Orowan stress is of the order of 2 MPa, much less than the flow stress [4, 5] (Fig. 1). It was concluded that the hardening was due to defect clusters which could not be observed in T.E.M.

CoO crystals annealed at very low oxygen pressure  $p_{\rm O_2}$  (see Sect. 2.1) have the lowest yield stress (Fig. 1). This is probably due to the absence of the defect clusters responsible for the hardening of asgrown and air annealed specimens [4, 5] (Fig. 1). Softening was observed for NiO after anneal at low  $p_{\rm O_2}$ , but the crystals contained a substantial amount of impurities [10]. The explanations for the softening/hardening behaviours of NiO and CoO are not the same.

The yield stress values obtained for the softest CoO are representative of materials containing almost no rate controlling obstacles;  $\tau_c$  is constant above 200 K (Fig. 1), with a value of 12 MPa slightly above the value of 8 MPa at 1 300 K [4]. Annealing in air increases the yield stress by  $\Delta \tau = 25$  MPa at room temperature (Fig. 1); for as-grown crystals,  $\Delta \tau$  is equal to 10 MPa. In region II, the values of

Fig. 3. — TEM observation of dislocations in CoO deformed at 4.2 K; engineering strain 1%. Foil parallel to the slip plane. The Burgers vector is parallel to g. Some magnetic domain walls are labelled m. Jog dragging events are shown by arrows.



Fig. 4. — An other area of the foil at large magnification. Many edge dipoles and multipoles can be observed.

 $\Delta \tau$  increase at lower temperature, corresponding to the thermally activated overcoming of obstacles by dislocations.

In region I,  $\Delta \tau = 40$  MPa for the two kinds of specimens tested (Fig. 1) and does not depend on temperature. The strengthening mechanism has no influence on the activation volume (Fig. 2) indicating that the defect clusters creates a long range athermal stress compared to the obstacles to dislocation glide. This, together with the values of  $v^*$  of the order of  $10 \ b^3$  (Fig. 2) is a strong suggestion to invoke the Peierls mechanism.

We analyse the data in region I using a standard theory [11]. The Peierls stress  $\tau_p$  is about 100 MPa (Fig. 1). This value is large  $(\tau_p \sim 6.5 \times 10^{-3} \, \mu$ ;  $\mu = (C_{11} - C_{12})/2 = 1.6 \times 10^{10}$  Pa) compared to those found for  $\{110\}$  slip in NaCl structure crystals [1, 12, 13] which are about 10 times smaller (MgO:  $\tau_p/\mu < 5 \times 10^{-4}$ ) in spite of the similar ionicity of the chemical bond [2]. Generally, it is found that the Peierls stress for screw dislocations is larger than for edges [16]. The deformation is then controlled by the motion of kinks on screw dislocations. We analyse our data with this assumption.

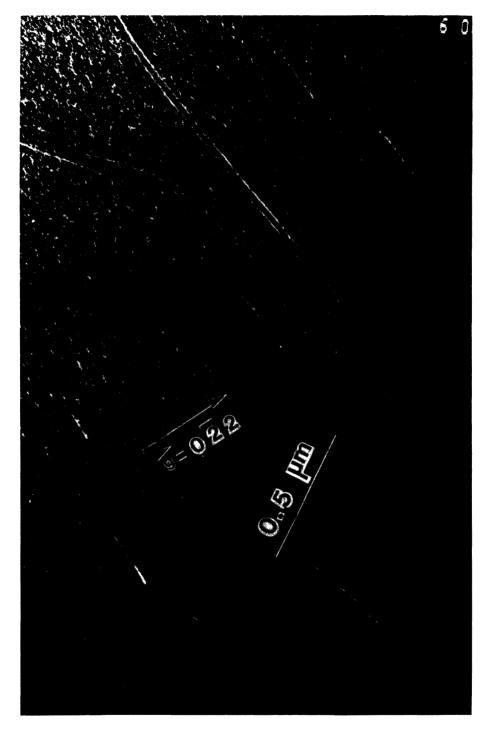


Fig. 5. — Weak beam dark field observation of an area next to the one of figure 4 with dipoles and multipoles. No dissociation for  $g = \pm 220$ .

The activation energy for kink pair formation at  $\tau = 0$  is given by:

$$H_0 = a \sqrt{ab\tau_p E_L};$$

where a is the period of the Peierls potential, b the Burgers vector and

$$E_{\rm L} = \frac{Kb^2}{4\pi} \log \frac{R}{b};$$

the line energy (see appendix for  $K=K_{\rm s}$  or  $K_{\rm e}$ ),  $R\sim 3~000~b$  the average distance between dislocations.

If screws were responsible of the experimental value of the Peierls stress  $\tau_{\rm p}=100$  MPa, one would find  $H_0^{\rm s}=2.5\times 10^{-20}$  J (0.15 eV). Conversely, one would find  $H_0^{\rm e}=5.2\times 10^{-20}$  J (0.32 eV) if  $\tau_{\rm p}$  was to be assigned to edges. The maximum temperature  $T_{\rm c}$  below which the Peierls mechanism operates is

given by  $H \sim 30~kT_{\rm c}$  (k= Boltzmann constant); one finds  $T_{\rm c}=59~{\rm K}$  for screws (126 K for edges). In view of the many approximations of the model, these values are estimates. It is clear that  $T_{\rm c}$  for screws corresponds to the experimental one (Fig. 1) which is 70 K. This does not disagree with our assumption for the analysis of experimental data. In many NaCl structure crystals, screw dislocations have also been shown to have a velocity lower than edges [2], and thus they control yielding.

The Peierls mechanism shows a reasonable fit with the mechanical data of region I (Figs. 1 and 2). However, the precipitates or defect clusters harden CoO in region I ( $\Delta \tau = 40$  MPa) more than in region II ( $\Delta \tau \sim 10$  MPa). It is not clear whether heat treated crystals still contain imperfection which are able to harden them; if it is the case, we can expect a residual  $\Delta \tau$  in region I which is larger than that observed in region II (Fig. 1). If we assume that, in region I, the residual  $\Delta \tau$  is 30 MPa, we can plot the  $\tau_c$  versus T curve for the Peierls mechanism, shown in figure 1 as a broken line. It can be fitted with an equation derived from models [1]. The Peierls stress in then  $\tau_p \sim 90$  MPa, larger than those of other NaCl structure crystals.

4.2 DISLOCATION MICROSTRUCTURE. — The most prominent feature of the dislocation microstructure is the observation of dipoles, largely with edge character (Figs. 3, 4 and 5). Although this microstructure is related to that during deformation at 4.2 K, it has certainly been modified during the heating up to room temperature. As shown in the appendix, under the applied load at 4.2 K, dipoles with a separation larger than 2.9 nm are unstable; this value is much smaller than the observed ones which range between 10 nm and 30 nm (see Sect. 3.2). These dipoles have not been formed during the deformation at 4.2 K. They are stable if they are not submitted to  $\tau$  which can be calculated with the help of the appendix. Separations between 10 and 30 nm give  $\tau'$  between 35 and 12 MPa (anisotropic elasticity). These values correspond to the flow stress at T in the range 60 K to 300 K where the dipoles could have been formed.

According to the Peierls mechanism (see Sect. 4.1), we expected to find, for a strain of 1 %, isolated dislocations along the Peierls Valleys, with a dominant screw character. We found no screw dislocation in the foils that we examined (Fig. 3). We conclude that extensive recovery occurs when the specimen is warmed up to room temperature after the mechanical test. This recovery involves dislocation glide and is activated by the internal stresses built up by the deformation at 4.2 K. Two mechanisms can be invoked:

(i) the microstructure is so similar to the one of NaCl structure crystals [2] that the same mechanism

could explain the formation of dipoles. In CoO, the double cross-slip could be helped by the presence of defect clusters. TEM observations on annealed crystals purposely deformed at room temperature should help to support this assumption;

(ii) an alternative explanation is that the energy stored by deformation at 4.2 K is reduced by dislocation rearrangement. We can expect that rectangular dislocation loops are formed during deformation at 4.2 K, with long screw segments and short edge ones. Interactions are strong enough to allow extensive motion at room temperature. Screw dislocations, which are not largely dissociated, easily cross-slip and annihilate; edge dipoles remain from the initial configuration. Their separation is dictated by stresses intermediate between the flow stress at 4.2 K and the one at 300 K, in agreement with observations (see Sect. 3.2).

It would be nice to avoid the recovery and observe the genuine low temperature microstructure. This could be done by pinning dislocations by irradiation [14], or by deforming at a flow-stress not too high compared with the one at room temperature.

#### 5. Conclusions.

CoO single crystals have been deformed down to 4.2 K; observations are analogous to those obtained for other NaCl structure crystals. By annealing at low oxygen pressure, it has been possible to obtain crystals with a minimum amount of precipitates or defect clusters. Their role on plastic flow, combined with the one of the Peierls mechanism is not yet fully understood. More TEM observations would be fruitful to give a thorough view of the mechanisms of low temperature deformation of CoO single crystals.

### Acknowledgments.

The authors are indebted to the LPMTM, Université Paris-Nord which provided the equipment for crystal growth. The cooperation between France and Spain is supported by the *action intégrée* n° 132.

## Appendix.

ELASTIC ANISOTROPY AND DISLOCATIONS. The elastic constants are known for CoO down to 250 K [15], about 40 K below the Néel temperature:

$$C_{11} = 19.5 \ C_{12} = 16.3 \ C_{44} = 8.1 (\times 10^{10} \, \mathrm{Pa}).$$

The anisotropy factor  $A = C_{44}/(C_{11} - C_{12})$  is 5.1, a rather large value. For T = 300 K, A = 1.4. We examine briefly how this can influence the dislocation behaviour in CoO.

Elastic energies of isolated dislocations. — For screw dislocations, the energy coefficient is given by:  $K_s = \sqrt{C_{44}(C_{11} - C_{12})/2}$ ; with the above values, we find:  $K_s = 3.6 \times 10^{10} \, \mathrm{Pa}$ .

For pure edge dislocations, using equation (13-161) in [16], we find :  $K_e = 5.7 \times 10^{10}$  Pa. The ratio  $K_e/K_s$  is  $(1 - \nu)^{-1}$  for isotropic media, i.e. at 300 K ( $\nu = 0.36$ )  $K_e/K_s = 1.55$  slightly smaller than  $K_e/K_s = 1.57$  at 250 K for anisotropy media. The elastic anisotropy has a limited influence on dislocations in the (110) [110] slip system.

Dipole formation. — Dipoles are stable if the local shear stress  $\tau$  results in a force on edge dislocations smaller than the maximum interaction force, given in isotropic elasticity by:  $0.25 \mu b^2/2 \pi (1 - \nu) y$  [17], where y is the distance between glide planes. The maximum  $y_{\rm M}$  is given by:

$$\frac{y_{\rm M}}{b} = \frac{0.25}{2 \pi (1 - \nu)} \frac{\mu}{\tau} \,. \tag{A1}$$

By taking an average shear modulus  $\mu = 5.5 \times 10^{10} \, \mathrm{Pa}$ ,  $\tau = 12 \, \mathrm{MPa}$  at 300 K (Fig. 1), one finds:  $y_{\mathrm{M}} = 285 \, b = 85 \, \mathrm{nm}$  ( $b = 0.3 \, \mathrm{nm}$ ). For a stress 10 times larger, we can expect  $y_{\mathrm{M}}$  10 times smaller. In CoO,  $\tau$  at 4.2 K is about 10 times larger than at 300 K. However, the crystal becomes largely anisotropic below 280 K; we therefore have to check if it influences the dipole equilibrium. The interaction force in the glide plane is proportional to the shear component  $\tau_{xy}$  of the stress field around and edge dislocation. It is given by equation (13-118) in [16]:

$$\frac{\tau_{xy}}{b} = \frac{K_{\rm e}}{2 \, \pi \rho^4} \left( -x^3 + \frac{\overline{C'}_{11}}{C'_{22}} x y^2 \right) \tag{A2}$$

We have taken the Burgers vector b along the x axis and the dislocation line along z. This requires to rotate the elastic constant matrix  $C_{ij}$  given in the cube axis. The new values  $C'_{ij}$  are:

$$C'_{11} = C_{11} + \frac{1}{2}H = 26 \times 10^{10} \,\mathrm{Pa}$$
;

with

$$H = 2 C_{44} + C_{12} - C_{11} = 13 \times 10^{10} \text{ Pa} ;$$
 
$$C'_{22} = C_{22} + \frac{1}{2} H = C'_{11} .$$

This gives:

$$\overline{C_{11}'} = \sqrt{C_{11}' C_{22}''} = C_{11}';$$

$$C_{66}' = C_{44} - \frac{1}{2}H = 1.6 \times 10^{10} \text{ Pa};$$

$$C_{12}' = C_{12} - \frac{1}{2}H = 9.8 \times 10^{10} \text{ Pa}.$$

x refers to the separation of dislocations in their glide plane,  $\rho$  is given by equation (13-119) in [16]:

$$\rho^4 = (x^2 + y^2)^2 + 11.2 x^2 y^2.$$
 (A3)

One can deduce from equation (A2) the equilibrium positions of the dipole given by  $\tau_{xy} = 0$ . They are identical to those found in the isotopic elasticity with

$$x = 0$$
 and  $x = \pm y$ .

We are now interested in finding the conditions for stability of dipoles. We, therefore, need the maximum interaction force, which corresponds to:

$$\frac{\partial \tau_{xy}}{\partial x} = 0 . (A4)$$

The equation (A4) reduces, after some algebra, to:

$$x^6 - 16.2 x^4 y^2 - 16.2 x^2 y^4 + y^6 = 0$$
 (A5)

which has four real roots:

$$x \simeq 4.14 \ y \ ;$$
  
 $x \simeq (4.14)^{-1} \ y \ .$ 

By substituting these values in equations (A2) and (A3), one finds a maximum  $y_{\rm M}$  for the stability of dipoles under a shear stress  $\tau$ . The two sets of roots give identical magnitude of  $y_{\rm M}$ . For  $\tau=12$  MPa (T=300 K), we have  $y_{\rm M}=29$  nm. This value is almost three times smaller than the one calculated for isotropic medium. At 4.2 K, the flow stress is 10 times larger; the maximum separation of dipoles formed under that flow-stress is 2.9 nm.

### References

- SUZUKI, T. and KOIZUMI, H., Int. Symp. on Lattice related properties of dielectric Materials (Turawa) 1985, pp. 117-130.
- [2] CASTAING, J., Ann. Phys. Fr. 6 (1981) 195.
- [3] APPEL, F. and WIELKE, B., *Mater. Sci. Eng.* **73** (1985) 97.
- [4] CASTAING, J., SPENDEL, M., PHILIBERT, J., DOMIN-GUEZ-RODRIGUEZ, A. and MARQUEZ, R., Revue Phys. Appl. 15 (1980) 277.
- [5] GUIBERTEAU, F., JIMENEZ-MELENDO, M., DOMIN-GUEZ-RODRIGUEZ, A., MARQUEZ, R. and CASTAING, J., Cryst. Lattice Defects Amorph. Mater. 16 (1987) 91.
- [6] SUZUKI, T. and KIM, H., J. Phys. Soc. Jpn 39 (1975) 1566.
- [7] DOTSENKO, V. I., Phys. Status Solid. B 93 (1979) 11.
- [8] REMANT, G., DELAVIGNETTE, P., LAGASSE, A. and AMELINCKX, S., *Phys. Status Solid.* 11 (1965) 329

- [9] COATES, P. J., EVANS, J. W. and WESTMACOTT, K. H., J. Mater. Sci. 17 (1982) 3281.
- [10] Dominguez-Rodriguez, A., Castaing, J. and Philibert, J., *Mater. Sci. Eng.* **27** (1977) 217.
- [11] GUYOT, P. and DORN, J., Can. J. Phys. **45** (1967) 983.
- [12] SUZUKI, T., SKROTZKI, W. and HAASEN, P., *Phys. Status Solidi B* **103** (1981) 763.
- [13] SKROTZKI, W. and SUZUKI, T., Radiat. eff. 74 (1983) 315.
- [14] MUGHRABI, H., J. Microsc. Spectrosc. Electron. 1 (1976) 571.
- [15] ALEKSANDROV, K. S., SHABANOVA, L. A. and RESHCHIKOVA, L. M., Sov. Phys. Solid State 10 (1968) 1316.
- [16] HIRTH, J. P. and LOTHE, J., Theory of dislocations, 2nd Edition (J. Wiley) 1982.
- [17] HULL, D. and BACON, D. J., Introduction to dislocations, 3rd Edition (Pergamon Press) 1984.